51st IEEE Conference on Decision and Control
December 10-13, 2012. Maui, Hawaii, USA

Bootstrap Current Optimization in Tokamaks Using Sum-of-Squares Polynomials

A. Gahlawat[1,2], E. Witrant[1], M. M. Peet[2], and M. Alamir[1]

Abstract— **In this paper we present a Lyapunov based feedback design strategy, by employing the sum-of-squares polynomials framework, to maximize the bootstrap current in tokamaks. The bootstrap current may play an important role in reducing the external energy input required for tokamak operation. The sum-of-squares polynomials framework allows us to algorithmically construct controllers. Additionally, we provide a heuristic to take into account the control input shape constraints which arise due to limitations on the actuators.**

I. INTRODUCTION

A tokamak is a device which uses toroidal and poloidal magnetic fields to heat and compress Deuterium-Tritium plasma in order to initiate and sustain a nuclear fusion reaction [16]. Toroidal and poloidal magnetic coils are combined to produce a helical magnetic field that confines the plasma. The poloidal field is also generated by the plasma current. The plasma current contributes to the plasma heating, and thus to the pressure distribution, as a consequence of the electrical resistance of the plasma [16].

The main source of current in a tokamak is the one induced in the plasma by the transformer action caused by the central ohmic coil [20]. This current is also known as the induced current. Additional sources of current are the radio-frequency (RF) antennas. The total current provided by these sources accounts for a considerable portion of energy required for tokamak operation. An additional source of current is internally generated by particles trapped between isoflux surfaces (surfaces with constant magnetic flux). This current is referred to as the bootstrap current [20]. Thus, bootstrap current is an automatically generated source of plasma current. An increase in the bootstrap current would lead to a reduced requirement of external current inputs provided by the transformer action and the RF-antennas. This reduced dependence on external current sources would also increase the pulse lengths for which the tokamak can operate. For example, the ultimate goal of the ITER project [8] is to demonstrate the steady state operation of tokamaks. A high value of bootstrap current has been identified as a crucial factor for steady state operation of tokamaks [10], [18].

The bootstrap current density is given by

$$j_{bs}(x,t) = C(x,t)\partial\psi/\partial x,$$

where $C(x,t)$ is a function of the pressure and temperature profiles of electrons and ions [21], $\psi(x,t)$ is the poloidal magnetic flux profile, $x \in [0,1]$ is the spatial variable and $t \geq 0$ is time. Additionally, $C(x,t)$ is continuous and bounded in both space and time and is non-zero on non-zero measure subsets of $[0,1]$ for all time. The dependence of the bootstrap current on poloidal flux, pressure and temperature profiles is explained in [9]. The goal of this paper is to enhance the bootstrap current density by constructing optimal controllers for the gradient of the poloidal flux using the RF-antennas. We achieve this goal by employing a simplified model for the evolution of $\partial\psi/\partial x$. Unfortunately, since j_{bs} appears in this model, the resultant model is a non-linear partial differential equation in $\partial\psi/\partial x$. To overcome this issue, we linearize j_{bs} about an operating point of $\partial\psi/\partial x$ and then use this linearized model to construct Sum-of-Squares-based controller-synthesis conditions which minimize the effect of disturbances on the norm of the state $\partial\psi/\partial x$. In addition, we also provide a heuristic to enforce spatial shape constraints on the control input. These constraints arise as a consequence of the actuators' operational limits.

The application of the sum-of-squares framework allows us to algorithmically construct controllers in a computationally effective manner. In [7] we used sum-of-squares polynomials to control the safety-factor profile [20] in tokamaks. We made the simplifying assumptions of considering both the bootstrap current and plasma resistivity to be static. These assumptions resulted in a linear partial differential equation model for the evolution of $\partial\psi/\partial x$. In this paper, we consider time varying plasma resistivity profile. Such resistivity profiles and the linearized j_{bs} result in a linear partial differential equation model of $\partial\psi/\partial x$ with time-varying distributed coefficients. Additionally, in the presented work we consider shape constrains on the control inputs, which we did not consider in [7]. Examples of control of tokamak plasmas with bootstrap current as a primary current source can be found in [10], [12]. A few additional research papers on the application of sum-of-squares polynomials for controller synthesis of infinite-dimensional systems are [15], [6].

The paper is organized as follows: Section II briefly covers the concepts used throughout the paper, Section III provides the main contribution and in Section VI we numerically simulate the controlled system and discuss the results.

The authors are with: [1] UJF / CNRS, Grenoble Image Parole Signal Automatique (GIPSA-lab), UMR 5216, B.P. 46, F-38402 St Martin d'Héres, France; [2] Cybernetic Systems and Controls Lab (CSCL) in the Department of Mechanical, Materials and Aerospace Engineering, Illinois Institute of Technology, Chicago,Il-60616, USA. E-mail: agahlawa@hawk.iit.edu

978-1-4673-2066-5/12/$31.00 ©2012 IEEE

II. PRELIMINARIES

A. Notation

The space $C_2^n[0,1]$ is defined to be the set of $n-$times continuously differentiable functions satisfying $\|f\|_{C_2^n[0,1]} = \left(\int_0^1 |f(x)|^2 dx\right)^{\frac{1}{2}} < \infty$.

For a given strictly positive polynomial M on $[0,1]$, we define the space $C_2^{n,M^{-2}}[0,1]$ to be the set of $n-$times continuously differentiable functions satisfying $\|f\|_{C_2^{n,M^{-2}}[0,1]} = \left(\int_0^1 |M^{-2}(x)f(x)|^2 dx\right)^{\frac{1}{2}} < \infty$.

We define the space $L_2((0,T);C_2^n[0,1])$, for $0 < T \leq \infty$, to be the set $n-$times continuously differentiable functions $f(t,x)$ with support on $x \in [0,1]$ and $t \in [0,T]$ satisfying $\|f\|_{L_2((0,T);C_2^n[0,1]} = \left(\int_0^T \|f(x,t)\|^2_{C_2^n[0,1]} dt\right)^{\frac{1}{2}} < \infty$.

The definition of the spaces $C_2^1((0,T);C_2^n[0,1])$ and $C_2^1((0,T);C_2^{n,M^{-2}}[0,1])$, for $0 < T \leq \infty$, follow similarly.

B. Dynamic Model of the Poloidal Flux Gradient

We employ the model presented in [21] for the evolution of the poloidal magnetic flux ψ. This model uses a cylindrical approximation and neglects the diamagnetic effect to obtain

$$\frac{\partial \psi}{\partial t}(x,t) = \frac{\eta_\parallel(x,t)}{\mu_0 a^2}\left(\frac{\partial^2 \psi}{\partial x^2} + \frac{1}{x}\frac{\partial \psi}{\partial x}\right) + \eta_\parallel(x,t) R_0 j_{ni}(x,t) \tag{1}$$

with the boundary conditions

$$\frac{\partial \psi}{\partial x}(0,t) = 0 \text{ and } \frac{\partial \psi}{\partial x}(1,t) = -R_0\mu_0 I_p(t)/2\pi,$$

where $I_p(t)$ is the plasma current, $\eta_\parallel(x,t)$ is the plasma resistivity, μ_0 is the permeability of free space, a is the radius of the last closed magnetic surface , R_0 is the plasma major radius and $j_{ni}(x,t)$ is the combined current density resulting from RF and bootstrap sources. Additionally, $x \in [0,1]$ is the spatial variable and $t \geq 0$ is the time.

To simplify notation, we begin by defining the variable $Z(x,t) = \psi_x(x,t)$[1]. To obtain an expression for the evolution of Z, we differentiate (1) in space to obtain

$$\frac{\partial Z}{\partial t}(x,t) = \frac{1}{\mu_0 a^2}\frac{\partial}{\partial x}\left(\frac{\eta_\parallel(x,t)}{x}\frac{\partial}{\partial x}\left(xZ(x,t)\right)\right) + R_0\frac{\partial}{\partial x}\left(\eta_\parallel(x,t) j_{ni}(x,t)\right)$$

with boundary conditions

$$Z(0,t) = 0 \text{ and } Z(1,t) = -R_0\mu_0 I_p(t)/2\pi. \tag{2}$$

The non-inductive current density $j_{ni}(x,t)$ is a sum of the external non-inductive current density $j_{eni}(x,t)$ and the bootstrap current density $j_{bs}(x,t)$. Separating these terms, the model can be represented as

$$\frac{\partial Z}{\partial t}(x,t) = \frac{1}{\mu_0 a^2}\frac{\partial}{\partial x}\left(\frac{\eta_\parallel(x,t)}{x}\frac{\partial}{\partial x}\left(xZ\right)\right) + R_0\frac{\partial}{\partial x}\left(\eta_\parallel(x,t) j_{bs}(x,t)\right) + R_0\frac{\partial}{\partial x}\left(\eta_\parallel(x,t) j_{eni}(x,t)\right). \tag{3}$$

In our analysis, we will assume that

$$Z_x(1,t) = -Z(1,t). \tag{4}$$

This assumption is based on the observation that the total current density $j_T(x,T)$, defined in [1] as

$$j_T(x,T) = -(xZ_x(x,t) + Z(x,t))/\mu_0 R_0 a^2 r$$

is weak at the plasma edge, however, we assume it to be zero.

Recall that by definition, $j_{bs}(x,t) = C(x,t)/Z(x,t)$, is a function of Z, where $C(x,t)$ is a function of the pressure and density profiles. As a result the PDE is implicitly nonlinear in the variable Z. We address this problem by linearization of $j_{bs}(x,t)$ about an operating point $\bar{Z}(x)$ to get

$$j_{bs}(x,t) = \bar{C}(x)/\bar{Z}(x) + u(x,t),$$

where $\bar{C}(x)$ corresponds to the static operating point $\bar{Z}(x)$ and $u(x,t) = (\partial C/\partial Z)|_{Z=\bar{Z}}(Z(x,t) - \bar{Z}(x))$. For our analysis, we take $\bar{C}(x)/\bar{Z}(x) = 0$. Simulation results, presented in Section VI verify that this assumption does not have a significant effect on the controller performance. At this point we would like to remark that even though we aim to solely minimize the norm of the Z-profile, in a more realistic setting, a feasible target Z-profile would have to be taken into account during control synthesis. This is due to the relationship between the safety factor profile and the poloidal magnetic flux gradient profiles [21]. Finally, the evolution model of $Z(x,t)$ used for the controller synthesis is

$$\frac{\partial Z}{\partial t}(x,t) = \frac{1}{\mu_0 a^2}\frac{\partial}{\partial x}\left(\frac{\eta_\parallel(x,t)}{x}\frac{\partial}{\partial x}\left(xZ\right)\right) + R_0\frac{\partial}{\partial x}\left(\eta_\parallel(x,t) j_{eni}(x,t)\right) + R_0\frac{\partial}{\partial x}\left(\eta_\parallel(x,t) u(x,t)\right). \tag{5}$$

We will take the disturbance $u(x,t)$ to be the external input to the system and assume that that $u \in L_2((0,\infty), C_2^2[0,1])$. This also implies that for all $0 < T < \infty$, $u \in L_2((0,T), C_2^2[0,1])$. Additionally, we will assume that for all initial conditions $Z_0 \in C_2^2[0,1]$ and all sufficiently smooth $\eta_\parallel$, there exists a unique solution $Z \in C_2^1((0,T);C_2^2[0,1])$ satisfying

$$\frac{dZ}{dt}(x,t) = \frac{1}{\mu_0 a^2}\frac{\partial}{\partial x}\left(\frac{\eta_\parallel(x,t)}{x}\frac{\partial}{\partial x}\left(xZ\right)\right) + R_0\frac{\partial}{\partial x}\left(\eta_\parallel(x,t) j_{eni}(x,t)\right) + R_0\frac{\partial}{\partial x}\left(\eta_\parallel(x,t) u(x,t)\right). \tag{6}$$

Refer to Section 7.6 in [14] for the existence and uniqueness of solutions to parabolic partial differential equations with time-varying evolution operators. Improved regularity of the solutions can be proven by using the approach presented in [5][2] wherein the authors prove the existence of smooth solutions of (3) for $j_{bs}(x,t) = j_{eni}(x,t) = 0$.

[1]Throughout the paper, for a function $f(x)$ of a variable x, $f_x(x)$ denotes the partial derivative of $f(x)$ with respect to x.

[2]For review purposes, a preprint is available at `http://www.gipsa-lab.fr/~e.witrant/papers/12_ACC_Bribiesca.pdf`

C. Control input

In system (5), the external non-inductive current density $j_{eni}(x,t)$ is the control input. The actuators for the control input are typically lower hybrid current density (LHCD) antennae and electron cyclotron current drive (ECCD) antennae. In this paper we consider actuation using a single LHCD antenna.

Using X-ray measurements from *Tore Supra*, an empirical model of current deposition was developed in [21]. This model uses a Gaussian deposition pattern with control authority over certain scaling parameters. In particular, we may use

$$j_{eni}(x,t) = v_{lh}(t)e^{-\frac{(\mu_{lh}(t)-x)^2}{2\sigma_{lh}(t)}}, \tag{7}$$

where we may control v_{lh}, μ_{lh} and σ_{lh} with the constraint that $v_{lh}(t) \in [0, 1.22\text{ MA}]$, $\mu_{lh}(t) \in [0.14, 0.33]$ and $\sigma_{lh}(t) \in [0.016, 0.073]$ for all $t \geq 0$.

In this paper, we will design control laws for these three input parameters using full-state feedback. This framework assumes that we can measure $Z(x,t)$ in real-time. Methods for estimating $Z(x,t)$ in real-time are discussed in [11]. Note that in the presented work, we choose the Gaussian parameters as the control input parameters and not the $N_\parallel$ and P_{LH}. This is a simplified approach, however, it must be noted that in a real tokamak, the two parameters $N_\parallel$ and P_{LH} determine the three Gaussian parameters and hence the mean, variance and amplitude of current deposits cannot vary independently.

D. Sum-of-squares polynomials

A polynomial $p(x)$ in variables $x \in \mathbb{R}^n$ is a sum-of-squares polynomial (SOSP) if there exist polynomials $p_i(x)$ for $i \in \{1, \cdots, N\}$ such that

$$p(x) = \sum_{i=1}^{N} p_i^2(x).$$

Any SOSP is non-negative. The following theorem provides a necessary and sufficient condition for a polynomial to be SOSP.

Theorem 1 ([13]): A polynomial $p(x)$, $x \in \mathbb{R}^n$ for $n \in \mathbb{N}$, of degree $2d$, $d \in \mathbb{N}$, is a SOSP if and only if there exists a positive semi-definite and symmetric Q such that

$$p(x) = z(x)^T Q z(x), \tag{8}$$

where $z(x)$ is a vector of all monomials in x of degree d or less.

If $p(x)$ is a symmetric matrix-valued polynomial of dimension r then we replace $z(x)$ with $z(x) \odot I_r$ where I_r is the identity matrix of dimension r.

The problem of checking whether a polynomial is sign-semidefinite is NP-hard [2]. However, as a consequence of Theorem 1, the problem of checking whether a polynomial is SOS is an LMI [3] and is therefore computationally tractable.

E. A boundedness condition on the system solution

In this paper we consider $Z(x,t)$ to be the system output and the disturbance $u(x,t)$ as the system input. In this subsection we show that for a bounded input, the system output is bounded.

Lemma 1: Consider the function

$$V(t) = \int_0^1 Z(x,t) f(x) M^{-1}(x) Z(x,t) dx,$$

where $f(x) = x^2$, $M(x) > 0$, for $x \in [0,1]$, is a polynomial and $Z(x,t)$ is the solution of the evolution equation (5) with $u \in L_2((0,\infty), C_2^2[0,1])$.

Then if

$$\frac{dV(t)}{dt} = \dot{V}(t) \leq \frac{1}{\gamma}\|u(x,t)\|^2_{C_2^2[0,1]} - \gamma \|Z(x,t)\|^2_{C_2^{2,M-2}[0,1]},$$

for all $t \geq 0$,

$$\|Z(x,t)\|^2_{C_2^1((0,\infty);C_2^{2,M-2}[0,1])} \leq \frac{1}{\gamma^2}\|u(x,t)\|^2_{L_2((0,\infty);C_2^2[0,1])} + \frac{V(0)}{\gamma}.$$

Proof: Since $u \in L_2((0,\infty), C_2^2[0,1])$, for all $0 < t < \infty$, $u \in L_2((0,T), C_2^2[0,1])$. Thus, from our assumptions there exists a unique $Z \in C_2^1((0,T); C_2^2[0,1])$ satisfying (6). Additionally,

$$\frac{\dot{V}(t)}{2} = \int_0^1 Z(x,t) f(x) M^{-1}(x) \frac{dZ(x,t)}{dt} dx.$$

Note that this is well defined as $dZ(x,t)/dt$ is given by (6) and $f(x)$ cancels out the singularity at $x = 0$ due to $1/x$.

Assume that the hypotheses of the theorem hold. Integrating

$$\dot{V}(t) \leq \frac{1}{\gamma}\|u(x,t)\|^2_{C_2^2[0,1]} - \gamma \|Z(x,t)\|^2_{C_2^{2,M-2}[0,1]}$$

in time from 0 to an arbitrary $0 < T < \infty$,

$$\|Z(x,t)\|^2_{C_2^1((0,T);C_2^{2,M-2}[0,1])} \leq \frac{1}{\gamma^2}\|u(x,t)\|^2_{L_2((0,T);C_2^2[0,1])} + \frac{V(0)}{\gamma}.$$

Taking the limit $T \to \infty$ gives us

$$\|Z(x,t)\|^2_{C_2^1((0,\infty);C_2^{2,M-2}[0,1])} \leq \frac{1}{\gamma^2}\|u(x,t)\|^2_{L_2((0,\infty);C_2^2[0,1])} + \frac{V(0)}{\gamma}.$$

This expression is well defined since $\|u(x,t)\|^2_{L_2((0,\infty);C_2^2[0,1])} < \infty$ and $V(0)/\gamma$ is a constant. ■

III. Main result

We now apply integration by parts to the condition in Lemma 1 to formulate our optimization problem which will allow us to synthesize controllers which minimize the upper

bound $\frac{1}{\gamma}$ on $Z(x,t)$. We assume that the plasma resistivity can be approximated, as given in [4][3]:

$$\eta_{\|}(x,t) = \mathbf{a}(t)e^{\lambda(t)x} \text{ for all } (x,t) \in [0,1] \times [0,T),$$

where $0 < \underline{a} \leq \mathbf{a}(t) \leq \bar{a}$ and $0 < \underline{\lambda} \leq \lambda(t) \leq \bar{\lambda}$.

Theorem 2: Suppose that for a given γ there exist polynomials $M, R : [0,1] \to \mathbb{R}$ such that $M(x) > 0$ for all $x \in [0,1]$, $\Omega(x,\lambda) + \Theta \leq 0$ for all $(x,\lambda) \in [0,1] \times [\underline{\lambda}, \bar{\lambda}]$ and $2A_4 + 2B_2 + A_2(1) \leq 0$, where $\Omega(x,\lambda) =$

$$\begin{bmatrix} 2A_1(x) & 0 & -R_0\mu_0 a^2 f(x) \\ 0 & A_0(x,\lambda) & -R_0\mu_0 a^2 f_x(x) \\ -R_0\mu_0 a^2 f(x) & -R_0\mu_0 a^2 f_x(x) & 0 \end{bmatrix},$$

$$\Theta = \begin{bmatrix} 0 & 0 & 0 \\ 0 & \frac{\mu_0 a^2 \gamma}{\underline{a}} & 0 \\ 0 & 0 & -\frac{\mu_0 a^2}{\bar{a}e^{\underline{\lambda}}\gamma} \end{bmatrix},$$

where

$$\begin{aligned} &A_0(x,\lambda) = 2A_3(x) - \lambda A_2(x) - A_{2,x}(x) + 2B_1(x,\lambda),\\ &A_1(x) = -f(x)M(x),\\ &A_2(x) = -\bar{f}(x)M(x) - f(x)M_x(x) - f_x(x)M(x),\\ &A_3(x) = -2M(x) - f_x(x)M_x(x), \quad A_4 = M(1),\\ &B_1(x) = -\frac{f_x(x)R(x)}{2} + \frac{f(x)R_x(x)}{2} + \lambda\frac{f(x)R(x)}{2},\\ &B_2 = \frac{R(1)}{2}, \quad f(x) = x^2 \text{ and } \bar{f}(x) = x. \end{aligned}$$

Then if

$$j_{eni}(x,t) = \frac{K(x)}{R_0\mu_0 a^2} Z(x,t)$$

where $K(x) = R(x)M^{-1}(x)$, then the effect of u on Z is bounded as follows.

$$\|Z(x,t)\|^2_{C_2^1((0,\infty);C_2^{2,M^{-2}}[0,1])} \leq \frac{1}{\gamma^2}\|u(x,t)\|^2_{L_2((0,\infty);C_2^2[0,1])} + \frac{V(0)}{\gamma}$$

Proof: Suppose that there exists a $\gamma > 0$ for which the hypotheses of Theorem 2 hold. Taking the time derivative of $V(t)$ gives us

$$\frac{\dot{V}(t)}{2} = \int_0^1 ZM^{-1}f\frac{dZ}{dt}dx = \dot{V}_1(t) + \dot{V}_2(t) + \dot{V}_3(t),$$

where

$$\begin{aligned} \dot{V}_1(t) &= \frac{1}{\mu_0 a^2}\int_0^1 ZM^{-1}f\frac{\partial}{\partial x}\left(\frac{\eta_{\|}}{x}\frac{\partial}{\partial x}(xZ)\right)dx,\\ \dot{V}_2(t) &= R_0\int_0^1 ZM^{-1}f\frac{\partial}{\partial x}(\eta_{\|}u)dx,\\ \dot{V}_3(t) &= R_0\int_0^1 ZM^{-1}f\frac{\partial}{\partial x}(\eta_{\|}j_{eni})dx. \end{aligned}$$

Note that we have dropped the spatial and temporal dependencies of the variables for brevity.

[3]For review purposes, a preprint is available at http://www.gipsa-lab.fr/~e.witrant/papers/12_TAC_Tokamak.pdf

We now define the new variable $Y(x,t) = Z(x,t)M^{-1}(x)$. Hence

$$\begin{aligned} \dot{V}_1(t) &= \frac{1}{\mu_0 a^2}\int_0^1 Yf\frac{\partial}{\partial x}\left(\frac{\eta_{\|}}{x}\frac{\partial}{\partial x}(xMY)\right)dx,\\ \dot{V}_2(t) &= R_0\int_0^1 Yf\frac{\partial}{\partial x}(\eta_{\|}u)dx \text{ and}\\ \dot{V}_3(t) &= R_0\int_0^1 Yf\frac{\partial}{\partial x}(\eta_{\|}j_{eni})dx. \end{aligned}$$

Applying integration by parts twice on $\dot{V}_1(t)$ we get

$$\begin{aligned} \dot{V}_1(t) &= \int_0^1 \frac{\eta_{\|}}{\mu_0 a^2}\left(Y_x A_1(x) Y_x\right)dx\\ &+ \int_0^1 \frac{\eta_{\|}}{\mu_0 a^2}\left(Y\left(A_3(x) - \frac{\lambda A_2(x)}{2} - \frac{A_{2,x}(x)}{2}\right)Y\right)dx\\ &+ \frac{\eta_{\|}(1)}{\mu_0 a^2}Y(1,t)\left(A_4 + \frac{A_2(1)}{2}\right)Y(1,t)\\ &+ \frac{\eta_{\|}(1)}{\mu_0 a^2}Z_x(1,t)Y(1,t). \end{aligned} \tag{9}$$

Here we have used the fact that

$$\begin{aligned} &Z(x,t) = M(x)Y(x,t)\\ &\Rightarrow Z_x(x,t) = M_x(x)Y(x,t) + M(x)Y_x(x,t)\\ &\Rightarrow Z_x(1,t) = M_x(1)Y(1,t) + M(1)Y_x(1,t). \end{aligned}$$

Due to the assumption on the total current density on the boundary $j_T(1,t)$ discussed in the prelimiaries and due to our linearization of j_{bs}, we obtain the boundary condition $u(1,t) = 0$. Applying integration by parts to $\dot{V}_2(t)$, we get

$$\dot{V}_2(t) = \int_0^1 R_0\eta_{\|}\left(Y(-f_x)u + Y_x(-f)u\right)dx \tag{10}$$

Using the feedback law $j_{eni}(x,t) = K(x)Z(x,t)/R_0\mu_0 a^2$, we get

$$\begin{aligned} \dot{V}_3(t) &= \frac{1}{\mu_0 a^2}\int_0^1 Yf\frac{\partial}{\partial x}\left(\eta_{\|}KZ\right)dx\\ &= \frac{1}{\mu_0 a^2}\int_0^1 Yf\frac{\partial}{\partial x}\left(\eta_{\|}KMM^{-1}Z\right)dx\\ &= \frac{1}{\mu_0 a^2}\int_0^1 Yf\frac{\partial}{\partial x}\left(\eta_{\|}RY\right)dx. \end{aligned}$$

Applying integration by parts twice, $\dot{V}_3(t)$

$$= \int_0^1 \frac{\eta_{\|}}{\mu_0 a^2}YB_1(x)Ydx + \frac{\eta_{\|}(1)}{\mu_0 a^2}Y(1,t)B_2Y(1,t). \tag{11}$$

Since $\dot{V}(t) = 2\dot{V}_1(t) + 2\dot{V}_2(t) + 2\dot{V}_3(t)$, using (9), (10) and (11), we obtain

$$\begin{aligned} \dot{V}(t) &= \int_0^1 \frac{\eta_{\|}}{\mu_0 a^2}\begin{bmatrix} Y_x \\ Y \\ u \end{bmatrix}^T \Omega(x,\lambda)\begin{bmatrix} Y_x \\ Y \\ u \end{bmatrix}dx\\ &+ \frac{\eta_{\|}(1)}{\mu_0 a^2}Y(1,t)\left(2A_4 + A_2(1) + 2B_2\right)Y(1,t)\\ &+ \frac{\eta_{\|}(1)}{\mu_0 a^2}Z_x(1,t)Y(1,t). \end{aligned}$$

Consequently,

$$\begin{aligned}
&\dot{V}(t) - \frac{1}{\gamma}\|u\|^2_{C_2^2[0,1]} + \gamma\|Z\|^2_{C_2^{2,M-2}[0,1]} \\
&= \dot{V}(t) - \frac{1}{\gamma}\|u\|^2_{C_2^2[0,1]} + \gamma\|Y\|^2_{C_2^2[0,1]} \\
&= \int_0^1 \frac{\eta_\|}{\mu_0 a^2} \begin{bmatrix} Y_x \\ Y \\ u \end{bmatrix}^T \Omega(x,\lambda) \begin{bmatrix} Y_x \\ Y \\ u \end{bmatrix} dx \\
&+ \int_0^1 \left(-\frac{u^2}{\gamma} + \gamma Y^2\right) dx \\
&+ \frac{\eta_\|(1)}{\mu_0 a^2} Y(1,t)\left(2A_4 + A_2(1) + 2B_2\right) Y(1,t) \\
&+ \frac{\eta_\|(1)}{\mu_0 a^2} Z_x(1,t) Y(1,t) \\
&= \int_0^1 \frac{\eta_\|}{\mu_0 a^2} \begin{bmatrix} Y_x \\ Y \\ u \end{bmatrix}^T \Omega(x,\lambda) \begin{bmatrix} Y_x \\ Y \\ u \end{bmatrix} dx \\
&+ \int_0^1 \frac{\eta_\|}{\mu_0 a^2} \left(-\frac{\mu_0 a^2 u^2}{\eta_\| \gamma} + \frac{\mu_0 a^2 \gamma Y^2}{\eta_\|}\right) dx \\
&+ \frac{\eta_\|(1)}{\mu_0 a^2} Y(1,t)\left(2A_4 + A_2(1) + 2B_2\right) Y(1,t) \\
&+ \frac{\eta_\|(1)}{\mu_0 a^2} Z_x(1,t) Y(1,t). \qquad (12)
\end{aligned}$$

Since $\eta_\|(x,t) = \mathbf{a}(t)e^{\lambda(t)x}$, $\underline{a} \le \eta_\|(x,t) \le \bar{a}e^{\bar{\lambda}}$ for all $(x,t) \in [0,1]\times[0,T)$. Hence,

$$\begin{aligned}
&\begin{bmatrix} Y_x \\ Y \\ u \end{bmatrix}^T \Omega(x,\lambda) \begin{bmatrix} Y_x \\ Y \\ u \end{bmatrix} - \frac{\mu_0 a^2 u^2}{\eta_\|\gamma} + \frac{\mu_0 a^2 \gamma Y^2}{\eta_\|} \\
&\le \begin{bmatrix} Y_x \\ Y \\ u \end{bmatrix}^T \Omega(x,\lambda) \begin{bmatrix} Y_x \\ Y \\ u \end{bmatrix} - \frac{\mu_0 a^2 u^2}{\bar{a}e^{\bar{\lambda}}\gamma} + \frac{\mu_0 a^2 \gamma Y^2}{\underline{a}} \\
&= \begin{bmatrix} Y_x \\ Y \\ u \end{bmatrix}^T (\Omega(x,\lambda) + \Theta) \begin{bmatrix} Y_x \\ Y \\ u \end{bmatrix}.
\end{aligned}$$

Since $\Omega(x,\lambda) + \Theta \le 0$ for all $(x,\lambda) \in [0,1]\times[\underline{\lambda},\bar{\lambda}]$, we conclude that

$$\begin{aligned}
&\int_0^1 \frac{\eta_\|}{\mu_0 a^2} \begin{bmatrix} Y_x \\ Y \\ u \end{bmatrix}^T \Omega(x,\lambda) \begin{bmatrix} Y_x \\ Y \\ u \end{bmatrix} dx \\
&+ \int_0^1 \frac{\eta_\|}{\mu_0 a^2} \left(-\frac{\mu_0 a^2 u^2}{\eta_\|\gamma} + \frac{\mu_0 a^2 \gamma Y^2}{\eta_\|}\right) dx \le 0 \qquad (13)
\end{aligned}$$

for all $t \ge 0$. Similarly, since from the theorem statement, we have $2A_4 + A_2(1) + 2B_2 \le 0$ and hence

$$\frac{\eta_\|(1)}{\mu_0 a^2} Y(1,t)\left(2A_4 + A_2(1) + 2B_2\right) Y(1,t) \le 0. \qquad (14)$$

Finally, from the boundary conditions given in (2) and (4) coupled with the definition of $Y(x,t)$, it is straightforward to observe that

$$\frac{\eta_\|(1)}{\mu_0 a^2} Z_x(1,t) Y(1,t) \le 0. \qquad (15)$$

Combining equations (12), (13), (14) and (15) we get

$$\dot{V}(t) \le \frac{1}{\gamma}\|u\|^2_{C_2^2[0,1]} - \gamma\|Z\|^2_{C_2^{2,M-2}[0,1]},$$

for all $t \ge 0$. Lemma 1 then completes the proof. ■

By using Sum-of-Squares to maximize γ in the conditions of theorem 2, we can minimize an upper bound on the state. Because bootstrap current is inversely proportional to Z and is non-zero on non-zero measure subsets of $[0,1]$ for all $t \ge 0$, this implies that our controller will maximize the bootstrap current.

IV. Constraints on the Controller Shape

The controller given by Theorem 2 will have a spatial distribution which is a function of the state $Z(x,t)$. Unfortunately, this distribution may not correspond with the Gaussian distribution described in our discussion of Subsection II-C. In order to constrain the input profile to have the required Gaussian shape, we propose the following simple heuristic.

To ensure that $j_{eni}(x,t)$ resembles a Gaussian defined by suitable choice of the time-varying parameters v_{lh}, μ_{lh} and σ_{lh}, we add an additional constraint to our optimization problem. This constraint has the form

$$g_1(x) \le j_{eni}(x,t) = \frac{K(x)}{R_0\mu_0 a^2} Z(x,t) \le g_2(x),$$

where $g_1(x) < g_2(x)$, for all $x \in [0,1]$, are polynomial approximations of two selected feasible Gaussians. Since both $K(x)$ and $Z(x,t)$ are continuous, the control input is a continuous function bounded by the the shape of the constraint envelope defined by $g_1(x)$ and $g_2(x)$. Additionally, we assume that

$$Z(x,t) = \alpha(t)Z_1(x) + (1-\alpha(t))Z_2(x) \text{ for all } t \ge 0,$$

where $\alpha \in [0,1]$ and $Z_1(x)$ is the polynomial approximation of the open-loop steady state. Similarly, $Z_2(x)$ is the polynomial approximation of the closed-loop steady state under maximum actuation of $j_{eni}(x,t) = j_{lh}(x,t)$. Hence, $Z_1(x)$ and $Z_2(x)$ define the expected envelope on the state $Z(x,t)$ established for a given set of operating conditions. The parameter α reflects our actuation capabilities. Since $K(x) = R(x)/M(x)$, the shape constraint becomes

$$\begin{aligned}
&R_0\mu_0 a^2 M(x) g_1(x) \le R(x)\left(\alpha Z_1(x) + (1-\alpha)Z_2(x)\right) \\
&\le R_0\mu_0 a^2 M(x) g_2(x)
\end{aligned}$$

for all $(x,\alpha) \in [0,1]\times[0,1]$. Although this approach is only a heuristic, we may improve our results by trying different constraint envelopes, as represented by $g_1(x)$ and $g_2(x)$.

V. Computation

Finally, we implement the conditions of Theorem 2 and the heuristic discussed previously using SOS. We formulate the optimization problem as follows. We are given polynomials $Z_1(x)$, $Z_2(x)$, $g_1(x)$ and $g_2(x)$ and solve the following.

Maximize $\gamma > 0$ such that following holds for some polynomials $M(x)$ and $R(x)$.

1) $M(x) > 0$ for all $x \in [0,1]$,

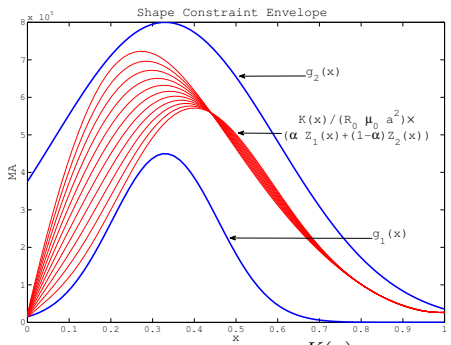

Fig. 1: Constraint envelope and $\frac{K(x)}{R_0\mu_0 a^2}(\alpha Z_1(x) + (1-\alpha)Z_2(x))$ for $\alpha \in [0,1]$

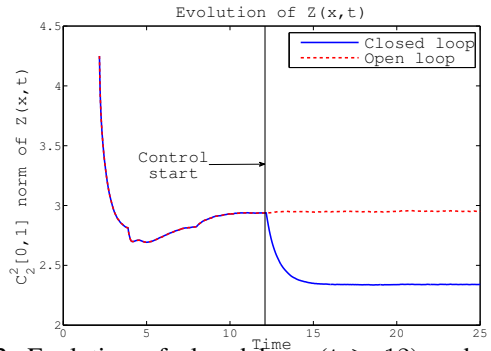

Fig. 2: Evolution of closed loop ($t \geq 12$) and open loop $\|Z(x,t)\|_{C_2^2[0,1]}$

2) $\Omega(x,\lambda) + \Theta \leq 0$ for all $(x,\lambda) \in [0,1] \times [\underline{\lambda}, \bar{\lambda}]$,
3) $2A_4 + 2B_2 + A_2(1) \leq 0$ and
4) for all $x \in [0,1]$ and $\alpha \in [0,1]$,

$$\begin{aligned} &R_0\mu_0 a^2 M(x) g_1(x) \\ &\leq R(x)\left(\alpha Z_1(x) + (1-\alpha)Z_2(x)\right) \\ &\leq R_0\mu_0 a^2 M(x) g_2(x) \end{aligned}$$

where $\Omega(x,\lambda)$, Θ, A_4, $A_2(x)$ and B_2 are defined in the statement of Theorem 2.

We solve the optimization problem using SOSTOOLS [17] toolbox for MATLAB©. The search for the maximum γ is performed using the bisection method. We solve this problem for the *Tore Supra* tokamak for which $R_0 = 2.38m$ and $a = 0.38m$. Moreover, the plasma resistivity is defined as $\eta_{\|}(x,t) = \mathbf{a}(t)e^{\lambda(t)x}$ where $\mathbf{a}(t) \in [0.0093, 0.0121]$ and $\lambda(t) \in [4, 7.3]$ for all $t \geq 0$. These values were obtained from the data for shot TS 35109.

VI. Simulation

We obtain a maximum value of $\gamma = 10^4$ as the solution for the optimization problem for *Tore Supra*. The feasible polynomials $M(x)$ and $R(x)$ obtained for this value of γ are of degree 12 in the spatial variable x. We simulate the closed-loop system on the simulator developed in [21]. This simulator considers the non-linear evolution model of $Z(x,t)$. The following figures provide the simulation results and show that although our controller was developed using a linearized model, it is effective in controlling the nonlinear PDE.

Figure 1 shows the constraint envelope as well as $\frac{K(x)}{R_0\mu_0 a^2}(\alpha Z_1(x) + (1-\alpha)Z_2(x))$ for several values of $\alpha \in [0,1]$, where $K(x) = R(x)/M(x)$.

Figure 2 shows the comparison between the time evolution of the spatial $C_2^2[0,1]$ norm of $Z(x,t)$ using both open-loop and closed-loop with closed loop control starting at $t = 12$. Figure 3 shows the evolution of the spatial L_2-norm of $j_{bs}(x,t)$ using both open-loop and closed-loop with closed loop control starting at $t = 12$. As a consequence of the decrease in $Z(x,t)$, we are able to obtain a percentage increase of $\approx 90\%$ in $\|j_{bs}\|_{L_2[0,1]}$.

Figure 4 illustrates the time evolution of the $j_{bs}(x,t)$ using level sets (shading).

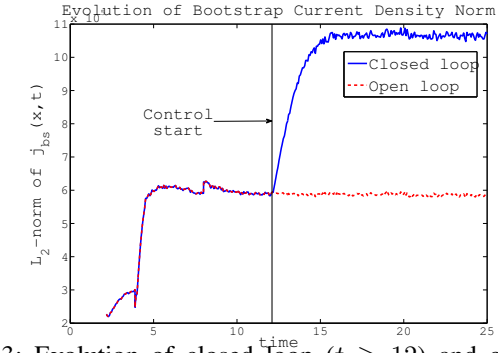

Fig. 3: Evolution of closed loop ($t \geq 12$) and open loop $\|j_{bs}(x,t)\|_{L_2(0,1)}$

Finally, to analyze the control input shapes, we fit a feasible Gaussian to control input at a time instance as shown in Figure 5. We observe that the control input approximates the shape of feasible Gaussians satisfactorily for roughly 70% of the spatial domain. However, the control input departs from the Gaussian shapes as $x \to 0$. This is due to the controller having the form $j_{eni}(x,t) = K(x)Z(x,t)/R_0\mu_0 a^2$ and the boundary condition $Z(0,t) = 0$. Note that the Gaussian approximation of the LHCD current deposit is obtained from hard X-ray measurements and, as stated in [21], a large uncertainty remains concerning the actual deposit close to the plasma center ($x = 0$). If a true zero boundary condition for the input is desired, then RF-antennas (ECCD) can be used to generate a sharper deposit profile near the plasma center.

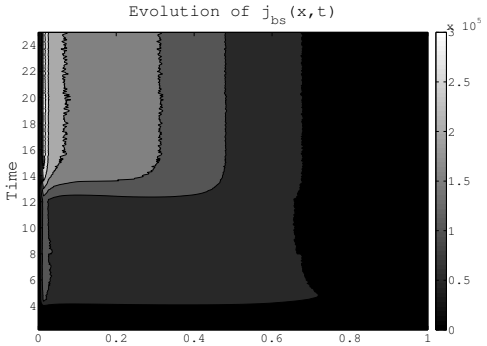

Fig. 4: Evolution of level sets of bootstrap current density $j_{bs}(x,t)$ in closed loop ($t \geq 12$)

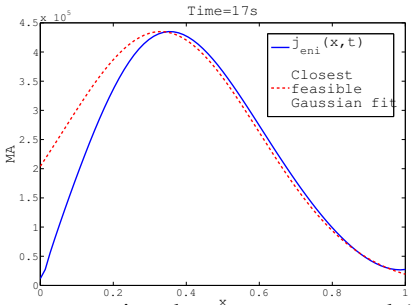

Fig. 5: Shape comparison between constructed $j_{eni}(x,t)$ and a feasible Gaussian with parameters $v_{lh} = 4.35 \times 10^5$, $\mu_{lh} = 0.33$ and $\sigma_{lh} = 0.072$ at a time instance of $17s$.

VII. Conclusions and Future Research

In this paper, we have investigated the use of the sum-of-squares (SOS) framework for the control of tokamak plasmas. In particular, we have devised a strategy to maximize the bootstrap current density in the plasma while taking into account the time varying plasma resistivity. Our method also provides a heuristic to constrain the shape of the control inputs. The simulation results illustrate the effectiveness of the proposed method.

Although the algorithms presented in this paper are effective at increasing bootstrap current, additional research must be performed before this method can be used to design controllers which can be tested under realistic operating scenarios. For example, in our approach, we assume that the controller gains are computed offline. This is based on a steady-state model of tokamak operation. It is possible that this model can be improved by gain-scheduling for different operating conditions. The next step towards controller implementation would be to design an online optimizer to infer the antennas' engineering parameters (power, refractive index for LHCD and orientation for ECCD) which minimize the difference between the desired and effective current deposit. We would also develop algorithms that return the values of engineering control parameters ($N_{\|}$ and P_{LH}) and not the Gaussian parameters since the engineering parameters are the control inputs for a tokamak. Additionally, we will devise conditions to show that the optimality condition on the state holds as long as there is a bounded difference between the desired and effective current deposit. In future work, we will also investigate the development of observer-based controllers which use bootstrap current density to estimate the state and controllers which take into account the coupling between Z and C. We will also need to validate our controllers on METIS [19], an advanced simulator for toroidal plasmas. Finally, we would also like to generalize our approach to include multiple LHCD and ECCD antennas.

VIII. Acknowledgements

This work was carried out within the framework of the European Fusion Development Agreement and the French Research Federation for Fusion Studies. It is supported by the European Communities under the contract of association between the European Atomic Energy Community (EURATOM) and CEA. The views and opinions expressed herein do not necessarily reflect those of the European Commission.

This research was carried out with the financial support of the Chateaubriand fellowship program and NSF CAREER Grant# CMMI-1151018.

References

[1] J. Blum. Numerical simulation and optimal control in plasma physics. 1989.

[2] L. Blum. *Complexity and real computation*. Springer Verlag, 1998.

[3] S. Boyd, L. El Ghaoui, E. Feron, and V. Balakrishnan. *Linear matrix inequalities in system and control theory*, volume 15. Society for Industrial Mathematics, 1994.

[4] F. Bribiesca Argomedo, C. Prieur, E. Witrant, and S. Brémond. A strict control lyapunov function for a diffusion equation with time-varying distributed coefficients. *Conditionally accepted for publication in IEEE Transactions on Automatic Control*, 2011.

[5] F. Bribiesca Argomedo, E. Witrant, and C. Prieur. Input-to-state stability of a time-varying nonhomogeneous diffusive equation subject to boundary disturbances. In *Proceedings of the 2012 American Control Conference*. AACC, 2012.

[6] A. Gahlawat and M.M. Peet. Designing observer-based controllers for pde systems: A heat-conducting rod with point observation and boundary control. In *Proceedings of the 50th IEEE Conference on Decision and Control, 2011*, 2011.

[7] A. Gahlawat, M.M. Peet, and E. Witrant. Control and verification of the safety-factor profile in tokamaks using sum-of-squares polynomials. In *Proceedings of IFAC World Congress, 2011*, volume 18, pages 12556–12561, 2011.

[8] BJ Green, I. Teams, et al. Iter: burning plasma physics experiment. *Plasma physics and controlled fusion*, 45:687, 2003.

[9] CE Kessel, TK Mau, SC Jardin, and F. Najmabadi. Plasma profile and shape optimization for the advanced tokamak power plant. *ARIES-AT, Fus. Eng*, 1980.

[10] M. Kikuchi. Steady state tokamak reactor based on the bootstrap current. *Nuclear fusion*, 30:265, 1990.

[11] D. Mazon, J. Blum, C. Boulbe, B. Faugeras, A. Boboc, M. Brix, P. De Vries, S. Sharapov, and L. Zabeo. Real-time identification of the current density profile in the jet tokamak: method and validation. In *Proceedings of the 48th IEEE Conference on Decision and Control, 2009 held jointly with the 28th Chinese Control Conference, 2009. CDC/CCC 2009.*, pages 285–290. IEEE, 2009.

[12] D. Moreau, F. Crisanti, X. Litaudon, D. Mazon, P.D. Vries, R. Felton, E. Joffrin, L. Laborde, M. Lennholm, A. Murari, et al. Real-time control of the q-profile in jet for steady state advanced tokamak operation. *Nuclear fusion*, 43:870, 2003.

[13] P.A. Parrilo. *Structured semidefinite programs and semialgebraic geometry methods in robustness and optimization*. PhD thesis, California Institute of Technology, 2000.

[14] A. Pazy. *Semigroups of linear operators and applications to partial differential equations*, volume 44. Springer, 1983.

[15] M. Peet, A. Papachristodoulou, and S. Lall. Positive forms and stability of linear time-delay systems. In *Proceedings of the 45th IEEE Conference on Decision and Control, 2006*, pages 187–193. IEEE, 2006.

[16] A. Pironti and M. Walker. Fusion, tokamaks, and plasma control: an introduction and tutorial. *Control Systems Magazine, IEEE*, 25(5):30–43, 2005.

[17] S. Prajna, A. Papachristodoulou, and P.A. Parrilo. Introducing sostools: A general purpose sum of squares programming solver. In *Proceedings of the 41st IEEE Conference on Decision and Control, 2002*, volume 1, pages 741–746. IEEE, 2002.

[18] KC Shaing, AY Aydemir, YR Lin-Liu, and RL Miller. Steady state tokamak equilibria without current drive. *Physical review letters*, 79(19):3652–3655, 1997.

[19] T. Takeda, K. Tani, T. Tsunematsu, Y. Kishimoto, G.I. Kurita, S. Matsushita, and T. Nakata. Plasma simulator metis for tokamak confinement and heating studies. *Parallel computing*, 18(7):743–765, 1992.

[20] J. Wesson. Tokamaks. Oxford University Press, New York, NY, 1987.

[21] E. Witrant, E. Joffrin, S. Brémond, G. Giruzzi, D. Mazon, O. Barana, and P. Moreau. A control-oriented model of the current profile in tokamak plasma. *Plasma Physics and Controlled Fusion*, 49:1075, 2007.